**Contract No:**

This document was prepared in conjunction with work accomplished under Contract No. 89303321CEM000080 with the U.S. Department of Energy (DOE) Office of Environmental Management (EM).

**Disclaimer:**

Savannah River National Laboratory®

# Optimization of CZTS Gamma-Ray Detectors

**Utpal N. Roy[1], Giuseppe S. Camarda[2], Yonggang Cui[2], Ge Yang[3] and Ralph B. James[1]**
[1]Savannah River National Laboratory, Aiken, SC 29808, USA.
[2]Brookhaven National Laboratory, Upton, NY 11973, USA.
[3]North Carolina State University, Raleigh, NC 27695, USA.

SPIE 2021

# Some benefits of Se in CdZnTe matrix

- **Strong influence in modifying Zn segregation coefficient: better compositional homogeneity with increased Se concentration for THM grown ingots.**
- **Effective solution hardening in arresting sub-grain boundaries and their network.**
- **Decreased Te-inclusion/precipitate concentration.**

# Factors to be considered for optimizing the CdZnTeSe composition

- Retrograde solubility of tellurium with Zn concentration variation
- Band-gap variation of the composition
- Role of Se on carrier trapping for point defects, complexes and any extended defects

# Phase diagram of CZT

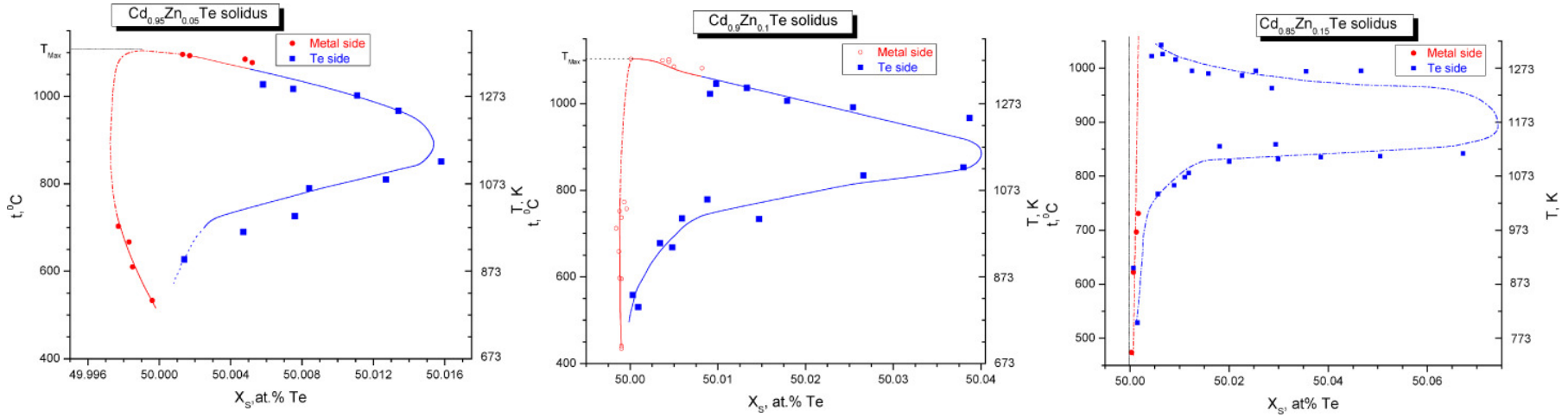


*T-X projection of $Cd_{0.95}Zn_{0.05}Te$, $Cd_{0.9}Zn_{0.1}Te$ and $Cd_{0.85}Zn_{0.15}Te$ solidus*

*Taken from V. N. Guskov et al., J. Alloys and Comp. 371 (2004) 118.*

**The peak position of the solidus curve shifts towards higher Te side for increased Zn concentration.**
**$X_s$= 50.015 Te for 5% Zn**
**$X_s$= 50.03% Te for 10% Zn and**
**$X_s$= 50.074% Te for 15% Zn.**

1. Higher Zn concentration: higher concentration of Te inclusions/precipitates.
2. Higher Zn concentration: higher alloy broadening.

# Band-gap variation of $Cd_{0.9}Zn_{0.1}Te_{1-y}Se_y$

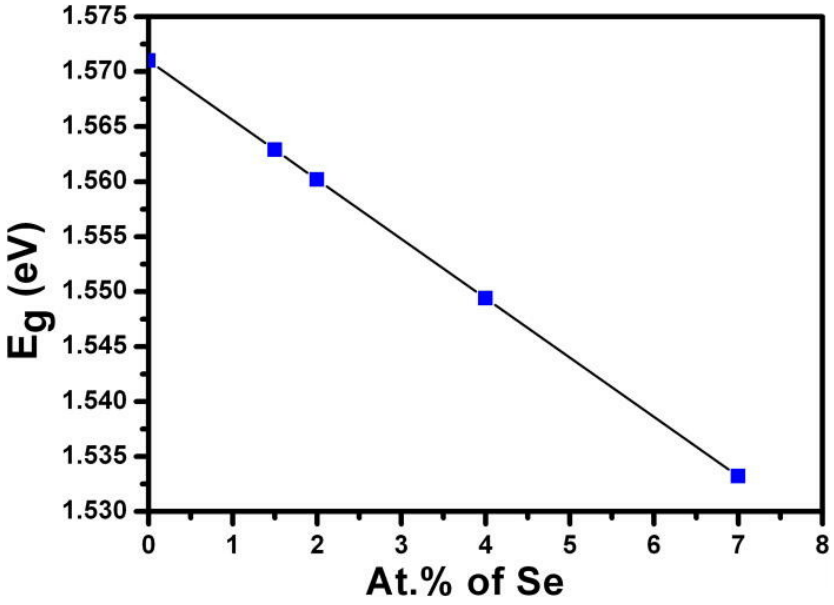


*Band-gap of $Cd_{0.9}Zn_{0.1}Te_{1-y}Se_y$ vs. selenium concentration.*

**As the band-gap in CZTS decreases with increased selenium concentration, there is a tradeoff in finding the minimum amount of selenium compound for acceptable resistivity and the optimum CZTS composition for the lowest performance limiting defects.**

# X-ray topography and IR transmission image of THM-grown $Cd_{0.9}Zn_{0.1}Te_{0.985}Se_{0.015}$

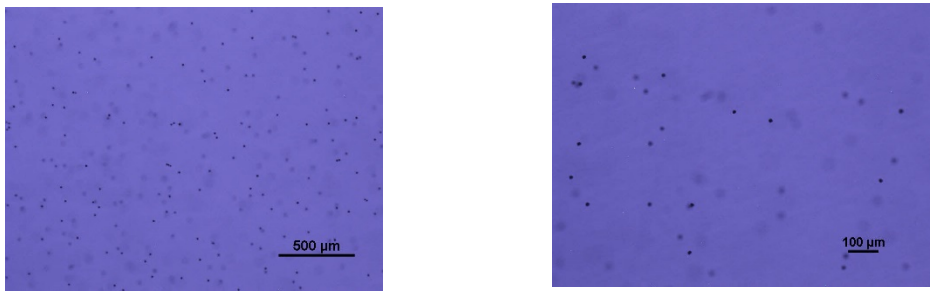


*High-magnification IR transmission microscopic images with two different magnifications.*

***The concentration and size of Te inclusions are comparable to as-grown CZT for CZTS with 1.5 atomic% of selenium. Thus. 1.5 atomic % of selenium composition is discarded, although the material is free from sub-grain boundary network.***

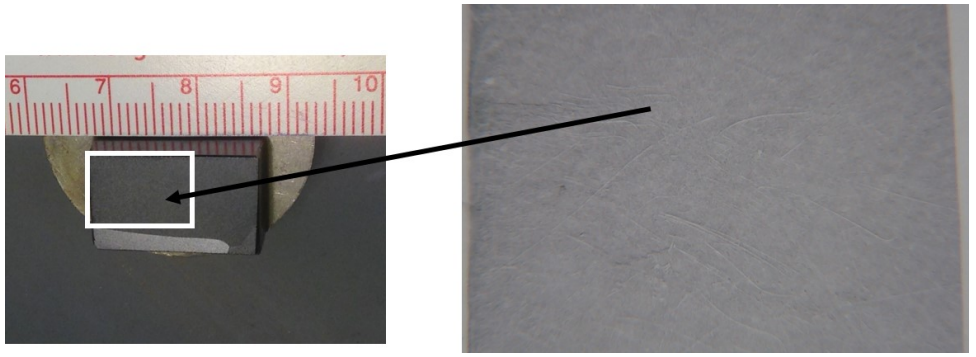


*Optical photograph and the corresponding X-ray topographic image of a $Cd_{0.9}Zn_{0.1}Te_{0.985}Se_{0.015}$ sample.*

# X-ray topography and IR transmission imaging of THM-grown $Cd_{0.9}Zn_{0.1}Te_{0.98}Se_{0.02}$

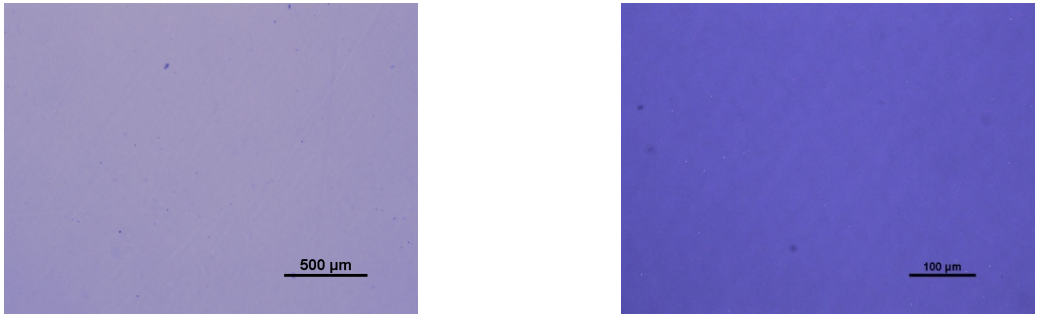


*High-magnification IR transmission microscopic images with two different magnifications.*

***The as-grown CZTS with 2 atomic% of selenium contains very low concentrations of Te inclusions. Additionally, the material is free from a sub-grain boundary network.***

***Apparently*** $Cd_{0.9}Zn_{0.1}Te_{0.98}Se_{0.02}$ **is the optimum composition with highly reduced performance limiting defects among the different compositions used in this study.**

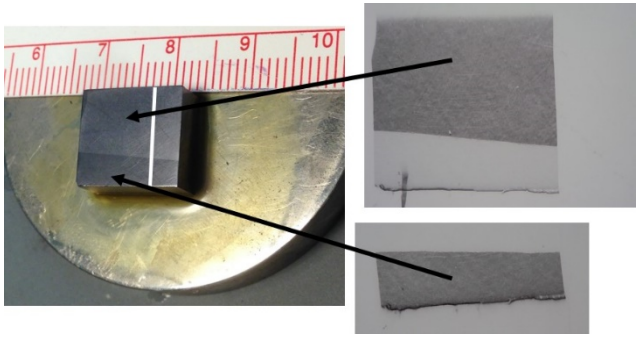


*Optical photograph and the corresponding X-ray topographic image of a* $Cd_{0.9}Zn_{0.1}Te_{0.98}Se_{0.02}$ *sample.*

# Qualitative evaluation of residual stress in CZTS

Two techniques are being used to evaluate the presence of residual stress in CZT qualitatively:

- X-ray topography: *Topographic image reveals structural deformation due to stress induced lattice-distortion.*
- IR transmission under crossed polarizers: *Stress-induced birefringence causes localized transmission of light through the sample.*

***Residual thermal stresses are responsible for a non-uniform electric field distribution and sub-grain boundaries. A uniform electric field is critically important to attain high performing radiation detectors. Thus, avoidance and/or mitigation of high thermal stress in the materials is a strict requirement for enhanced detector performance.***

# X-ray topography of CZTS

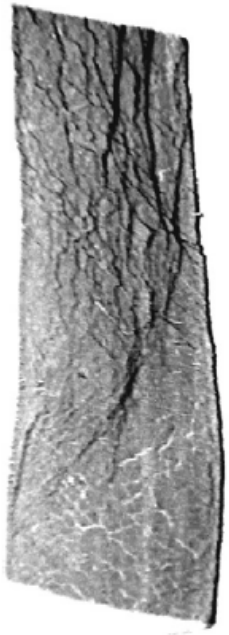

**X-ray topography of CZT Frisch-grid detector sample. Sample dimensions: 6x6x15 mm$^3$.** *(A. E. Bolotnikov et al., J. Cryst. Growth 379 (2013) 46)*

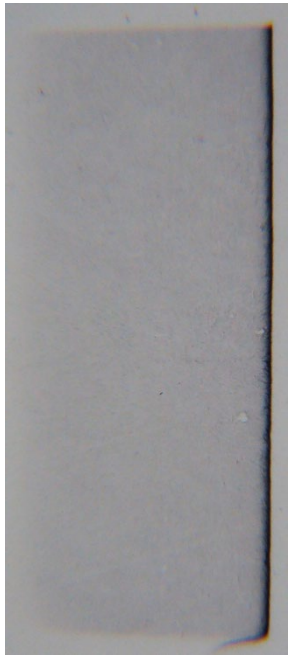

**Typical X-ray topography of THM grown CZTS (2% Se) Frisch-grid detector sample. Sample dimensions: 4.4x4.4x10 mm$^3$.**

***No deformation of the X-ray topographic image of CZTS sample with 2% Se. CZTS samples found to be almost free from residual stress as well as sub-grain boundary network.***

# X-ray topography of CZTS (contd.)

**Severe lattice distortion resulting from strain introduced by the crucible wall is very common for CdTe and CZT.**

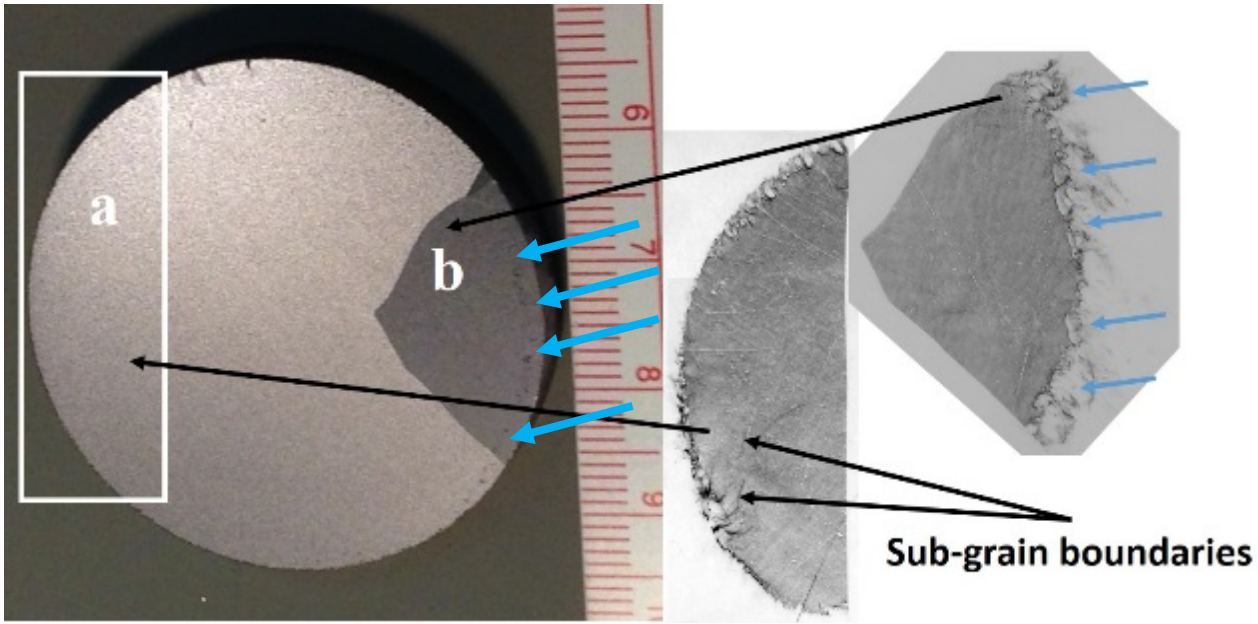


*Shape of the grain in the topographic image is unaltered. This indicates the absence of overall thermal stress in the wafer. The streaky nature of the periphery of grain b apparently indicates severe lattice distortion in the region indicating thermal stress. However, this streaky nature in the topographic image might be due to the pores/Te-inclusions near the periphery of the wafer as indicated by the blue arrows on the wafer picture.*

**Photograph of a 4-cm diameter Bridgman grown $Cd_{0.9}Zn_{0.1}Te_{0.93}Se_{0.07}$ lapped wafer cut perpendicular to the ingot axis and the X-ray topographic images of the region denoted by the white rectangle and the grain on the right side of the wafer.**

# X-ray topography of CZTS (contd.)

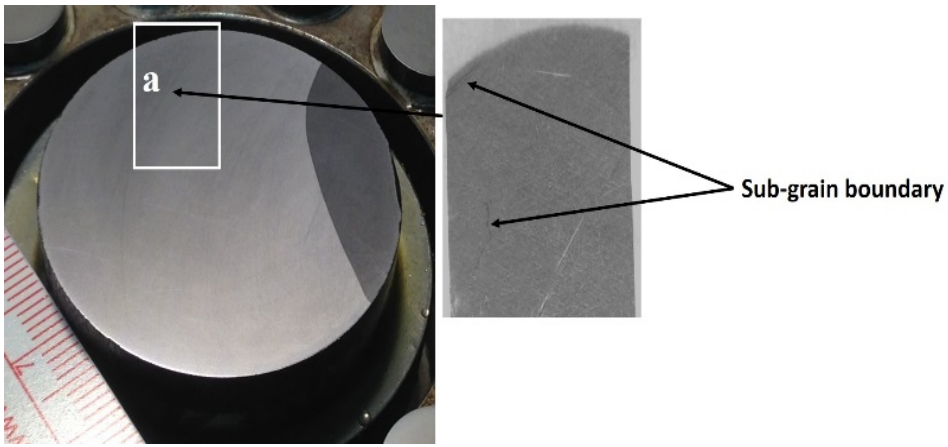


**Photograph of the 4-cm diameter Bridgman grown $Cd_{0.9}Zn_{0.1}Te_{0.93}Se_{0.07}$ lapped wafer cut perpendicular to the ingot axis and the X-ray topographic images of the region denoted by the white rectangle.**

***No severe lattice distortion near the periphery of the wafer was observed in the X-ray topographic image.***

# IR transmission under crossed polarizers

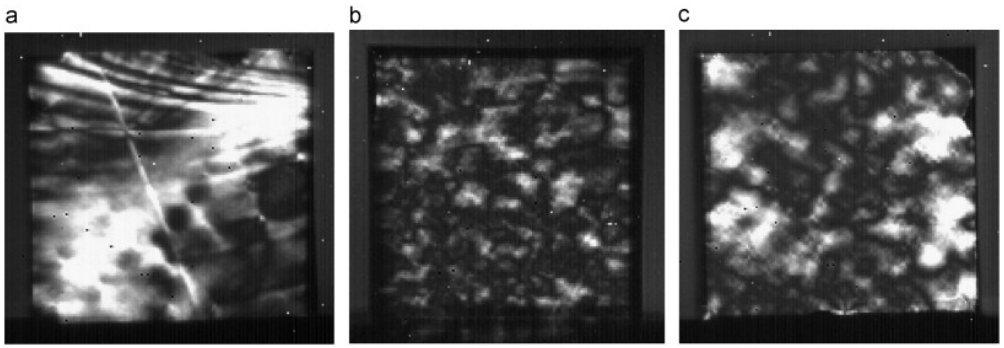


*Cross polarized IR transmission images of three different THM-grown CZT samples , with 100-mm² field of view.*
*S.A. Awadalla et al., J. Cryst. Growth 312 (2010) 507.*

Anode

Cathode

**Under crossed polarizers, zero volt  Under crossed polarizers, +2.5KV**

*Cross polarized IR transmission images of THM-grown CZTS (2% Se) Frisch-grid detector sample. Sample dimensions: 4.4x4.4x10 mm³.*

**Cross polarized IR transmission image reveals the absence of residual stress in CZTS samples.**

***CZTS samples did not show the presence of residual thermal stress.***

# Efficacy of Se addition in CZT matrix

- Enhanced compositional uniformity (about 90% of the ingot length)
- About 1.5 times increase of hardness as compared to CZT
- Reduced thermal stress
- Drastic reduction of Te inclusions
- Substantial reduction of sub-grain boundary and free from sub-grain network

# Charge Transport Properties of THM-grown CZTS with optimum 2% Se

***Composition:*** $Cd_{0.9}Zn_{0.1}Te_{0.98}Se_{0.02}$

***Resistivity:*** $1\text{-}3 \times 10^{10}\ \Omega\text{-cm}$

$\mu\tau_e$ **:** $4.5\text{-}5 \times 10^{-3}\ cm^2/V$ *(average),* $6.6 \times 10^{-3}\ cm^2/V$ *(highest)*

***Detector performance:***
***(~1-cm long Frisch grid detectors)***

*Energy resolution is 0.9-1.1 % at 662 keV,*
*best resolution achieved: ~0.77 % at 662 keV.*

**The composition with 2% Se ($Cd_{0.9}Zn_{0.1}Te_{0.98}Se_{0.02}$) was found to be *the best in terms of material properties and charge transport characteristics.***

# Present limitation of CZTS

We believe there is still room to further develop CZTS material and detector performance as we have observed relatively high concentrations of Cr, Fe, Ni, and Cu present in THM-grown $Cd_{0.9}Zn_{0.1}Te_{0.98}Se_{0.02}$ ingot at <20 ppba, 42 ppba, <4 ppba and 22 ppba (parts per billion atomic) respectively. CdSe is perhaps the source of the high concentrations of extrinsic impurities. The above impurities were not detectable in commercial CZT as analyzed by GDMS technique, except for Fe (at 22 ppba). [*J.J. McCoy et al., J. Electronic Materials 48, 4226 (2019).*]

***We expect to improve the energy resolution (as measured) at 662 keV to between 0.5-0.6 % for THM-grown $Cd_{0.9}Zn_{0.1}Te_{0.98}Se_{0.02}$ by using purified starting material.***

## Acknowledgement

**This work was supported by U.S. Department of Energy/NNSA, Office of Defense Nuclear Nonproliferation Research and Development. The author UNR acknowledges partial support of LDRD funding from SRNL.**

Thank you for your kind attention !